Effect of Changes in TiO_2 Dispersion on Its Measured Photocatalytic Activity

Terry A. Egerton* and Ian R. Tooley

School of Chemical Engineering and Advanced Materials, University of Newcastle, Newcastle Upon Tyne, NE17RU United Kingdom

Received: December 17, 2003

This paper reports measurements of photocatalytic oxidation of 2-propanol by dispersions of three different types (a high area rutile, a surface treated rutile, and, the mainly anatase, Degussa P25) of titanium dioxide in 2-propanol. For a fixed loading of any one type of TiO_2, the particle dispersion was deliberately modified by milling the suspension to break down the clusters of individual crystals which are usually present in dispersions of all inorganic powders. Sedimentation analysis demonstrated that, as predicted, milling decreased the size of the TiO_2 particles and this led to corresponding changes in the optical properties of their dispersions. Measurements of 2-propanol oxidation demonstrated that, for all three forms of titania, milling-times of 30 min led to an 80% decrease in the rate of acetone formation. We propose that the measured decrease is a consequence of the demonstrated increase in UV absorption associated with the reduction of particle size caused by milling. This increased absorption causes the UV flux incident on the catalyst slurry to be absorbed within a shorter path length, i.e., is absorbed by fewer crystals, say $1/F$ of the original number. Therefore, although the total number of charge-carriers generated by a fixed UV flux is constant, more (F times as many) charge-carriers/crystal are generated within a smaller number ($1/F$) of crystals. However, since electron−hole recombination statistics are bimolecular, if the photon absorption per crystal increases by some factor, F, the number of hydroxyl radicals generated in each crystal increases not by a factor F, but only by $F^{0.5}$. Because the number of hydroxyl radicals generated, the number of radicals/crystal multiplied by the number of crystals, varies as $F^{0.5} \times (1/F)$ and the total hydroxyl radical generation rate varies as $F^{-0.5}$. Since experimental measurements reflect the total rate of hydroxyl radical generation, the acetone production rate decreases as the UV absorption increases. This explanation of these counter-intuitive changes is relevant to *all* reactions carried out using semiconductor catalyst particles dispersed in a liquid. It is of special relevance to the many comparisons of the photoactivity of different types of TiO_2.

Introduction

Titanium dioxide is the most widely studied semiconductor photocatalyst.[1−3] Often it is necessary to minimize its photocatalytic activity, e.g., to reduce degradation of organic paint films by TiO_2 pigment[4,5] or avoid photooxidation of the visible-light harvesting dyes in TiO_2-based photovoltaic cells.[6] However, since TiO_2 is the leading contender for photo-catalyzed oxidation of both organic[1,7,8] and micro-biological contaminants,[8−10] most published research seeks to maximize its photochemical efficiency, which is generally limited by fast recombination of photogenerated electrons and holes, to <5%.[4,11,12] Consequently, programs to develop a technology based on TiO_2 photo-catalyzed destruction of pollutants seek either to increase the intrinsic photocatalytic activity or to minimize the economic consequences of low efficiency, e.g., by optimizing the UV source. This paper is central to both of these aims.

As part of the many attempts to understand, and hence maximize, the photocatalytic activity of TiO_2, the effects of crystal structure,[13,14] of surface area,[15] particle size,[16,17] and hydroxyl group density[18] of sol−gel[19] and gas-phase production methods,[20] dopants,[16,21] and the influences of surface modification[22] have all been investigated. However, even though changes in crystal structure, particle-size, and aggregation will affect the optical properties of the resulting dispersions, there has been little examination of how the optics of the TiO_2 dispersions influences measured activity. Those studies that that have been made, focus on the effects of wavelength[14,23] and UV intensity[4,24] on the measured photoactivity.

Therefore, this study seeks to investigate the effects of deliberate changes in the dispersion of TiO_2 slurries on their measured photocatalytic activity. The particle dispersion has been modified, by milling the titanium dioxide to break down the clusters, whether flocculates or aggregates, of individual crystals which are normally present in dispersions of inorganic powders.[25] Our chosen measure of photocatalytic activity has been the photooxidation of 2-propanol. Photooxidation of 2-propanol has been extensively studied in the gas phase,[26] pure liquid,[4,13,24] and 2-propanol/water solutions.[24,27] In all cases, acetone is the dominant product. The reaction is relatively well understood and can be studied in simple apparatus.

The accepted mechanism of 2-propanol photooxidation is the UV generation of electron−hole pairs followed by the interaction of the positive holes with either surface hydroxyl ions or hydroxyl ions in solution to form hydroxyl radicals. Thus

$$TiO_2 + UV \rightarrow e^- + h^+$$

$$e^- + O_2 \rightarrow O_2^-$$

$$h^+ + OH_s^- \rightarrow OH^\bullet$$

The consumption of oxygen has been directly demonstrated by

* To whom correspondence should be addressed. Tel: 0191 222 5618. Fax: 0191 222 5472. E-mail: t.a.egerton@ncl.ac.uk.

10.1021/jp0378992 CCC: $27.50
Published on Web 03/26/2004

TABLE 1: Titanium Dioxide Samples Used for the Photocatalytic Oxidation of Isopropanol to Acetone

sample	sample origin	surface area ($m^2\ g^{-1}$)	particle diameter (nm) based on area	crystal form	surface treatment
A	Uniqema	140	10	rutile	none
B	Tayca−MT100T	76	19	surface treated rutile	aluminum stearate
C	Degussa−P25	50	30	mainly anatase	none

Fraser and MacCallum[27] and formation of O_2^- has been monitored by chemiluminescence probing.[28] The hydroxyl radical, whose generation at the TiO_2 surface has been demonstrated by esr spin trapping,[29] then abstracts the α H from the alcohol[30] to initiate a reaction sequence that leads to acetone formation. A simple kinetic treatment[4] predicts that acetone formation rate varies as $k_s[KI/k_r]^{0.5}$ where I is the UV intensity, K is the rate of absorption of UV photons, k_r is the rate constant for electron−hole recombination (dependent on the number of recombination centers in the TiO_2 crystal), and k_s is the rate constant for the slowest surface reaction. The dependence of measured oxidation rate on $I^{0.5}$ demonstrated by Egerton and King has since been confirmed by a number of authors.[12,24,31]

Experimental Details

Materials. The titanium dioxide samples used, listed in Table 1, were selected to test the generality of our results and include a high area rutile, A, a surface treated rutile, B, and a (predominantly) anatase sample, C. Sample A, is an experimental rutile supplied by Uniqema, and sample B is an example of a commercially available surface treated (Tayca M100T) material. Both of these rutiles are believed to be manufactured by an aqueous precipitation method. Sample C, Degussa P25, is mainly anatase and is prepared by a high-temperature flame method and is included because of its widespread use in photocatalytic research. The surface areas were derived from BET analysis of low temperature (77 K) nitrogen adsorption isotherms for samples outgassed at 110 °C.

TiO_2/2-propanol dispersions were made either by hand-stirring the required amount of catalyst with 2-propanol (50 mL) or by using a small scale attritor-mill, Figure 1, to disperse the catalyst. This mill is designed to breakdown titanium dioxide aggregates in particulate dispersions without causing crystal fracture. The PTFE insert at the base of the mill pot prevents dead-spots in which pockets of unmilled slurry can form.

A known weight of titanium dioxide, typically 0.4 g, in 40 mL of 2-propanol was introduced to the mill pot, and 50 g of 180−212 μm solid soda-glass ballotini (Grade 11 Jencons Scientific Ltd) was then added. The suspension was then agitated by the impeller at 900 rpm. During this period, the agitated glass ballotini collide with the TiO_2 particles in suspension and break up any aggregates of primary crystals. After milling for a defined time, the impeller was stopped, and the ballotini were separated from the catalyst suspension and were washed with 2-propanol. The washings were then added to the suspension and the total volume adjusted to 50 mL.

Photooxidation Measurements. The photocatalytic generation of acetone by a known amount of catalyst dispersed in 2-propanol (50 mL) was measured in a cylindrical Pyrex reactor as shown in Figure 2.

The TiO_2/2-propanol suspension was illuminated, from below, by two Philips PL-L 36W 09 actinic lamps. The relative wavelength distribution of the light (measured with a Spex Radiometer) before passing through the heat filter is shown in Figure 3. The depth of TiO_2 dispersion varied from 4.5 cm at the start of the reaction to ~3.0 cm at the end of the reaction.

Prior to reaction, the reactor was equilibrated at 304 ± 1 K, and the contents were sparged with a constant flow of oxygen.

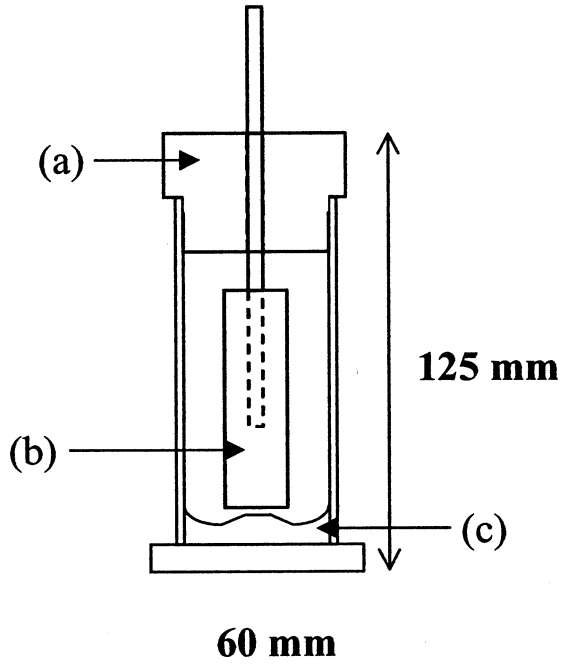

Figure 1. Small scale sand mill. (a) PTFE stopper, (b) polyurethane rubber impeller, and (c) PTFE insert.

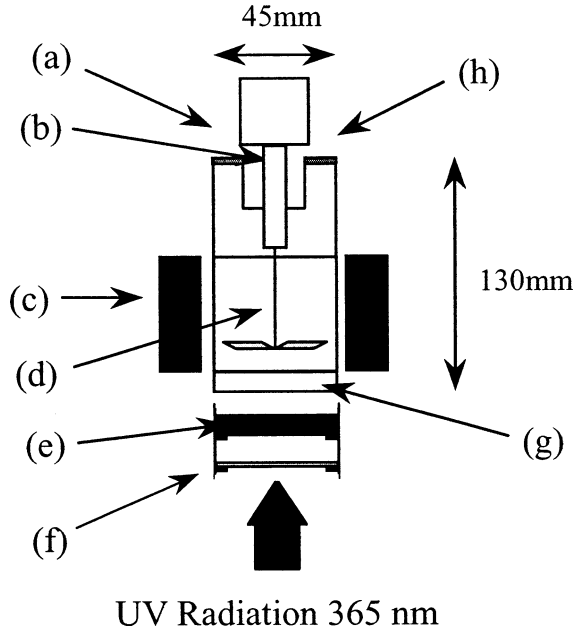

Figure 2. 2-Propanol oxidation reactor in which a suspension of titanium dioxide in 2-propanol could be irradiated from below by two horizontally positioned 36 W lamps. (a) Oxygen sparge, (b) sample port, (c) temperature control unit, (d) glass stirrer, (e) heat filter (10 cm^3 water), (f) optional optical density filter (Oreal), (g) calcium fluoride window, and (h) exhaust port.

During the reaction, the dispersion was continuously stirred, and a flow of oxygen was slowly bled across the dead volume. Samples of the reaction mixture were withdrawn by a hypodermic syringe through a port fitted with a septum cap and were then filtered through 2 μm PTFE filters to adequately remove

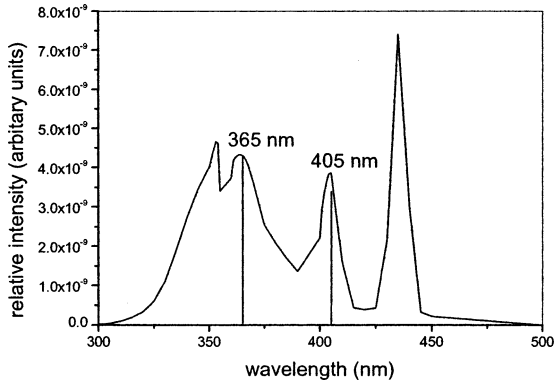

Figure 3. Spectral output Philips PL-L 09 36W 09 actinic lamps.

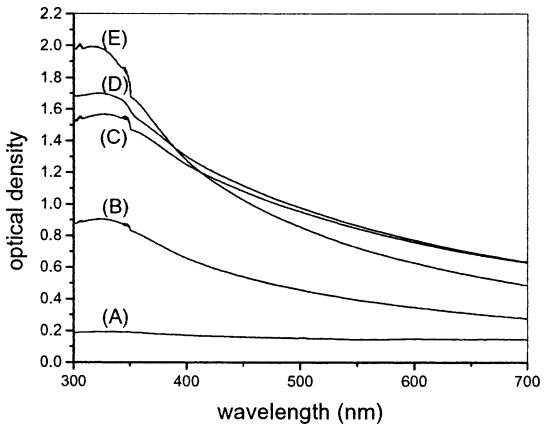

Figure 4. Transmission spectra of diluted (25-fold) suspensions of the high area rutile sample, A, (8 g dm^{-3} in 2-propanol) that had been milled for increasing time. (A) 0 min milling, (B) milled for 7.5 min, (C) milled for 15 min (start of experiment, time = 0 min), (D) milled for 15 min (end of experiment, time = 60 min), and (E) milled for 30 min.

titanium dioxide. The acetone content was analyzed on a gas chromatograph (Cambridge GC94: Chromosorb wax 60/80 mesh column at 70 °C) previously calibrated with acetone/2-propanol mixtures using a diethyl ether internal standard. Straight line calibration plots (R^2 0.997) were obtained.

Before starting a reaction, a sample (1 cm^3) of the dispersion was taken from the reactor and diluted to 100 cm^3 with 2-propanol. The 300−700 nm spectrum of the diluted suspension was then measured in 1 cm path length cells. Figure 4 shows the results for sample A and demonstrates that the optical properties of the suspension have been significantly altered by the changes in dispersion caused by milling. Corresponding spectra, measured at the end of the photooxidation runs, showed negligible change and thus demonstrated that during the reactions no significant change had occurred in the state of dispersion of the suspension.

Particle Size Measurements. The particle size distribution of selected dispersions was measured in a disk centrifuge (Brookhaven Instruments Corporation Model B1-XDC). In this instrument, the size distribution is deduced from the rate of particle sedimentation, induced by spinning the disk at known speeds (900−4500 rpm). The sedimentation is monitored by measuring the attenuation of a collimated X-ray beam. As it was not possible to make these measurements on 2-propanol dispersions, they were made on aqueous suspensions milled with a sodium silicate dispersant. In a typical experiment, the mean particle size (i.e., the size for which the mass percent undersize was 50%) of sample A, milled for 30 min, was 29 nm and 90% of the mass was below 45 nm. This compares with an estimate

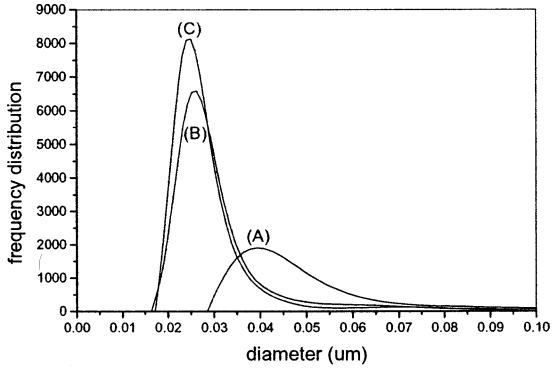

Figure 5. Particle size distributions measured in a Brookhaven disk centrifuge (Brookhaven Instruments Corporation model B1-XDC) of diluted suspensions of aluminum stearate coated sample A that had been milled for increasing time. (A) 0 min milling, (B) milled for 1 mill pass, and (C) milled for 8 mill passes.

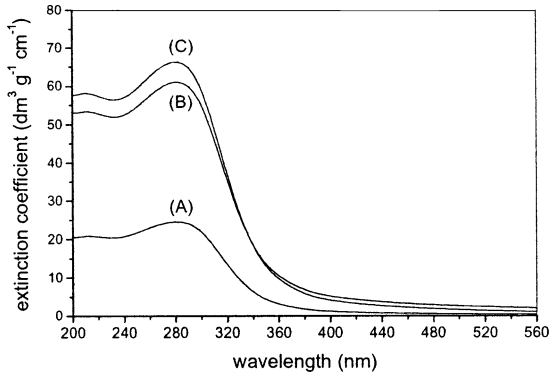

Figure 6. Transmission spectra of diluted suspensions of aluminum stearate coated sample A that had been milled for increasing time. (A) 0 min milling, (B) milled for 1 mill pass, and (C) milled for 8 mill passes.

of ∼10 nm derived from surface area measurements or ∼7 nm measured by X-ray line broadening. However, the TiO_2 particle size in dispersions that had not been milled was much larger. In one case (sample A surface treated with silica[22]), the particle size decreased from 1000 to 70 nm after 30 min of milling. A sample similar to B decreased from 55 to 28 nm after milling for 8 passes in a laboratory scale Netzsch mill, Figure 5.

All of these results are completely consistent with the interpretation, expressed above, that the changes in optical transmission (Figure 6) associated with milling the 2-propanol suspensions are the result of changes in the size of the TiO_2 particles in suspension.

Results

Preliminary experiments confirmed (Figure 7) that acetone formation from 2-propanol requires both UV irradiation and TiO_2 catalyst and established (Figure 8) the effect of catalyst loading on the measured rate of acetone formation in unmilled catalyst/2-propanol dispersions. On the basis of these results, a loading of 0.4 g per 50 mL (8 g dm^{-3}) was selected as the standard concentration for further experiments, since the measured rate is then relatively insensitive to small variations in the TiO_2 level, such as might occur if traces remained on the glass ballotini used in the milling.

The effect of milling on the formation of acetone on irradiation of suspensions of high area rutile, A, is shown in Figure 9. As the milling time increased from 0 to 30 min, the acetone-formation rate decreased by a factor of 4. A similar decrease in activity on milling was obtained for the surface-

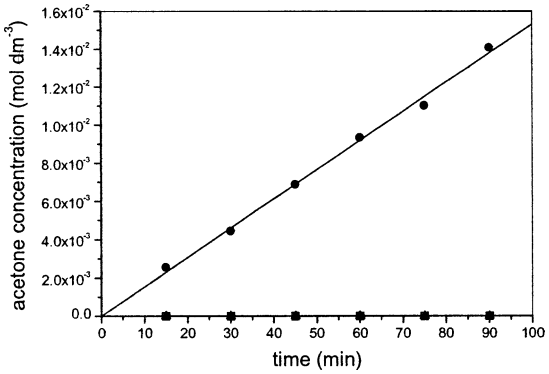

Figure 7. Results for sample A confirm that the formation of acetone requires both UV irradiation and TiO_2 catalyst. ● high area rutile sample A + 2-propanol + UV light + O_2, □ high area rutile sample A + 2-propanol + O_2 and ▲ 2-propanol + UV light + O_2. Reactions were carried out at 20 g dm^{-3} TiO_2 in 2-propanol.

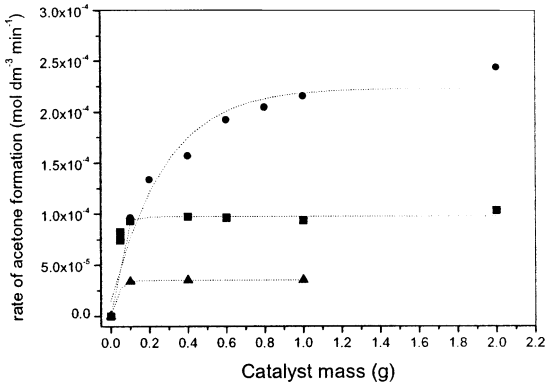

Figure 8. Effect of mass of unmilled high-area uncoated rutile, A, ●; surface-treated rutile, B, ▲; and (mainly) anatase sample, C, ■ on the measured rate of acetone formation.

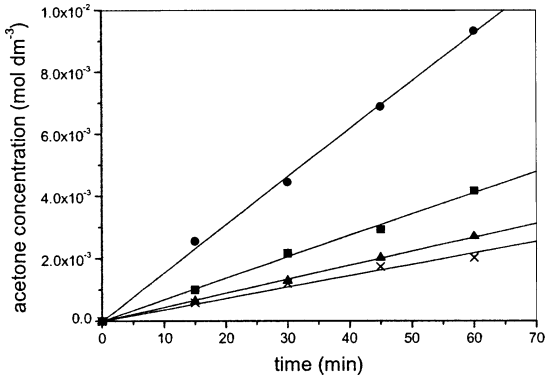

Figure 9. Effect of milling on the formation of acetone on irradiation of suspensions of high area rutile, A. ●; unmilled, ■; milled for 7.5 min, ▲; milled for 15 min and 5; milled for 30 min.

treated rutile sample B and the mainly anatase sample C, as shown in Table 2 and Figure 10. Thus, for all three samples, anatase and rutile, untreated and surface-coated, milling significantly reduced the measured rates of acetone production. As similar results have been obtained for three other, lower area (7−20 m^2 g^{-1}) TiO_2 samples (not reported here for reasons of brevity), the result appears to be a general one.

Discussion

An analysis of the effects of milling on the measured rates of photocatalysis by titanium dioxide suspensions must differentiate between primary particles (identified as ∼7 nm from

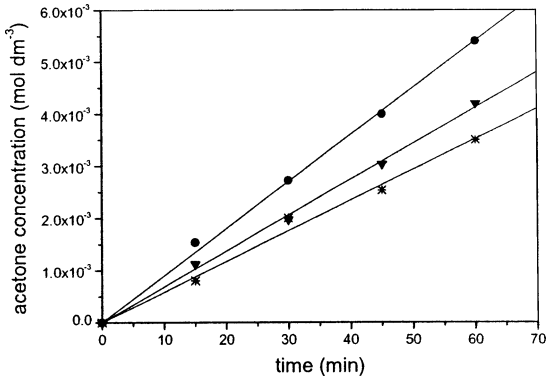

Figure 10. Effect of milling on the formation of acetone on irradiation of suspensions of (mainly) anatase sample C. ●; unmilled, ▼; milled for 90 min, *; milled for 180 min.

TABLE 2: Effect of Increased Milling of Titanium Dioxide Samples on the Measured Rate of Formation of Acetone

sample	BET area (m^2 g^{-1})	milling time (min)	10^5 × rate (mol dm^{-3} min^{-1})	rate relative to unmilled sample
A, rutile	140	0	15.4	1
A, rutile		7.5	6.85	0.45
A, rutile		15	4.46	0.29
A, rutile		30	3.62	0.24
B, rutile + stearate	76	0	3.54	1
B, rutile + stearate		7.5	2.57	0.72
B, rutile + stearate		30	2.27	0.64
C, mainly anatase	50	0	9.02	1
C, mainly anatase		90	6.86	0.76
C, mainly anatase		180	6.16	0.68

X-ray line broadening or ∼10 nm from surface area measurements) and the secondary particles formed when primary particles cluster together. These larger particles, variously described in the literature as agglomerates, aggregates, or flocculates, will hereafter be called aggregates. Because the attractive forces between TiO_2 particles are particularly large (a consequence of TiO_2's large Hamaker constant), secondary particles of TiO_2 are robust and not easily broken down into their primary constituents. Although this facilitates separation of TiO_2 nanoparticles from suspension, it makes their subsequent dispersion in liquids difficult. Even during the high shear regimes experienced during conventional milling of TiO_2 pigment,[32] breakdown of the aggregates is slow. Similarly, the slow reduction in the mean aggregate-size during dispersion of titanium dioxide in 2-propanol is central to the discussion of the photooxidation results. It might be supposed that milling the TiO_2/2-propanol suspensions would increase the accessible surface area and thus increase measured photocatalytic activity. However, the central point of this paper is that for all three, widely different, types of TiO_2 described above (and also for the three other unreported lower area examples), milling decreased the measured rate of photocatalysis. The largest decrease was for the uncoated rutile nanoparticles, A, for which the greatest aggregation of primary particles would be expected and least for the stearate coated rutile, sample B, for which least aggregation would be expected. Heller and co-workers have also measured the photocatalytic activity of TiO_2 as a function of milling.[15] However, their measurements were made on pigmentary TiO_2, 0.2 μm particles which had been ball milled (by dense alumina cylinders 6 mm diameter and 6 mm length) for extended periods of time (days), and for the reasons amplified below, we do not consider their interpretation of their results to be relevant to the much more lightly milled suspensions used in these studies.

TABLE 3: Estimated Distance within Which 90% of the Incident Radiation Is Absorbed by 8 g dm^{-3} Suspensions of High Area Rutile, Sample A, Milled for Increasing Times

milling time (min)	distance for 90% absorption of 325 nm radiation (cm)	distance for 90% absorption of 350 nm radiation (cm)	distance for 90% absorption of 375 nm radiation (cm)	distance for 90% absorption of 400 nm radiation (cm)
0	0.22	0.22	0.23	0.24
7.5	0.044	0.048	0.054	0.061
15	0.024	0.025	0.028	0.031
30	0.020	0.024	0.027	0.030

Both scattering and absorption of radiation, wavelength λ, by suspensions of particles, diameter d, are a function of d/λ and relative refractive index μ.[33,34] Because the UV wavelength (~350 nm) is larger than the primary-particle size of ~10 nm and the radiation responds to the aggregates, not the primary particles, the relevant d is that of the aggregates. Figure 4 shows that when, during the preparation of TiO_2/2-propanol suspensions for photocatalytic experiments, aggregates are broken down, causing d to decrease, the optical properties of the suspension change. Figures 5 and 6 directly demonstrate the changes in particle size distributions and optical properties of a stearate coated sample, similar to B, milled in water. Although fears of possible damage to the disk centrifuge by 2-propanol precluded particle-size measurements of samples milled in 2-propanol, optical measurements confirmed corresponding, though slower, changes when stearate coated samples were milled in 2-propanol. Overall the conclusion is clear: milling breaks down the aggregates and causes a significant change in the optics of the TiO_2 dispersions. The stability of the optical transmission curves with time (Figure 4) shows that, once achieved, particle size distributions are stable over the time of the photocatalytic experiments.

The optical properties of suspensions of particles of the type considered in these experiments, for which the ratio of $d/\lambda > 0.1$, are described by Mie[34] (and for the special case of TiO_2 by authors such as Tunstall[35]) and shown to be a function of both d/λ and the (complex) refractive index, μ. The Mie equations, as normally solved for the real part of the refractive index, predict the scattering of radiation as a function of particle size. The corresponding solutions for the imaginary part of the refractive index describe absorption of radiation and, through d/λ, define the dependence of absorption on particle size. The decreased 350 nm transmission on milling, Figure 4, is due to the increased absorption and scattering which Mie theory predicts will accompany reduction in particle size. Since separate calculations by Tunstall[35] suggest that the effects of changed particle size on the scattering and absorption coefficients roughly parallel one another, the measured changes in the transmission spectra are taken as a measure of increased UV absorption.

As summarized in the Introduction, the mechanism of 2-propanol oxidation by titanium dioxide has been extensively studied,[4,13,24,26,27] and it was demonstrated that the rate of 2-propanol oxidation varies as the square root of the UV intensity, ($I^{0.5}$) a consequence of the dominant effect of electron hole recombination. Increased UV absorption results in the incident photons being absorbed in a shorter path length of the suspension, i.e., by a smaller number of crystals, say $1/F$ of the original number. Each crystal acts as a nanoreactor and the consequence of absorption in a shorter path length is a reduction in the number of nanoreactors involved in photooxidation. To compensate for this, each of the nanoreactors absorbs more UV and the generation of charge carriers is correspondingly increased, tending to compensate for the decreased number of nanoreactors. i.e., $1/F$ crystals each absorbs F times as many photons. However, because of charge-carrier recombination, the rate per crystal does not increase pro rata, but only as $F^{0.5}$. Because of this, the compensation is incomplete and the total number of hydroxyl radicals varies as $(1/F) \times F^{0.5}$; that is, as $F^{-0.5}$, the result is an overall reduction in oxidation rate as the sample is milled and the UV is absorbed in shorter path lengths.

A fully quantitative analysis based on the above arguments requires a direct measurement of the UV absorption by the particles and must take into account both the wavelength distribution of the incident radiation and the variation of the imaginary part of the refractive index (the absorption) with wavelength. Our measurements, in a conventional spectrometer, of UV transmission do not differentiate between scattering and absorption. However, in the suspensions used by us photons are multiply scattered. Although at any one photon/particle interaction the chances of absorption and scattering are approximately equal, most scattered photons will interact with a second particle at which there is a further chance of absorption, and so on. Therefore, the measured transmission, although not an exact measurement of absorption, is a reasonable approximation to it. We therefore base our model on this approximation.

The rate of reaction in an element at a distance x into the suspension is given by $r_x = KI_x^{0.5}$ where $K = k_s[k_I/k_R]^{0.5}$ where k_I is the rate at which photons are absorbed, k_s is the rate of reaction of holes at the surface, and k_R is the rate of electron hole recombination.[4] The measured catalytic activity, R, may then be found by integrating the rate over the distance, x, penetrated by UV. Since $I_x = I_0 e^{-x/l}$ where I_0 is the incident intensity and I_x is the attenuated intensity at some distance x into the suspension $I_x^{0.5} = I_0^{0.5} e^{-x/2l}$, and therefore

$$R = \int_0^\infty r_x \, dx = \int_0^\infty KI_x^{0.5} \, dx = \int_0^\infty KI_0^{0.5} e^{-x/2l} \, dx = K_c \int_0^\infty e^{-x/2l} \, dx \quad (1)$$

where $K_c = KI_0^{0.5}$, and therefore

$$R = K_c[-2le^{-x/2l}]_0^\infty = K_c 2l \quad (2)$$

where l is the distance of UV penetration into the reaction cell. In a well milled system, A, the photons are absorbed in a short distance l_A, whereas in a poorly milled system, B, the UV penetrates a greater distance l_B and

$$\frac{R_A}{R_B} = \frac{l_A}{l_B} \quad (3)$$

The penetration depth, taken to be the path length corresponding to an absorbance of 1 (the path length in which 90% of the UV light is absorbed), was then estimated from the transmission values (measured at lower concentrations) of the different suspensions. The results at 325, 350, 375, and 400 nm for the particular case of sample A are shown in Table 3.

It can be seen that the calculated penetration depths decrease by a factor of 8 (at 400 nm) to 11 (325 nm) as milling proceeds. The corresponding rates of oxidation in the milled suspensions relative to those in the unmilled suspension were calculated and listed in Table 2. The calculations assume that the variations in

TABLE 4: Estimated Oxidation Rates, Assuming Equal Quantum Efficiencies for 325, 350, 375, and 400 nm Radiation, of Suspensions (8 g dm^{-3}) of High Area Rutile, Sample A, Milled for Increasing Times

milling time (min)	experimental rate (mol dm^{-3} min^{-1})	$10^5 \times$ rate calculated on the basis of 325 nm absorption (mol dm^{-3} min^{-1})	$10^5 \times$ rate calculated on the basis of 350 nm absorption (mol dm^{-3} min^{-1})	$10^5 \times$ rate calculated on the basis of 375 nm absorption (mol dm^{-3} min^{-1})	$10^5 \times$ rate calculated on the basis of 400 nm absorption (mol dm^{-3} min^{-1})
0	15.4 (base figure for calculation)				
7.5	6.9	3.0	3.4	3.6	3.9
15	4.5	1.7	1.8	1.9	2.0
30	3.5	1.4	1.7	1.8	1.9

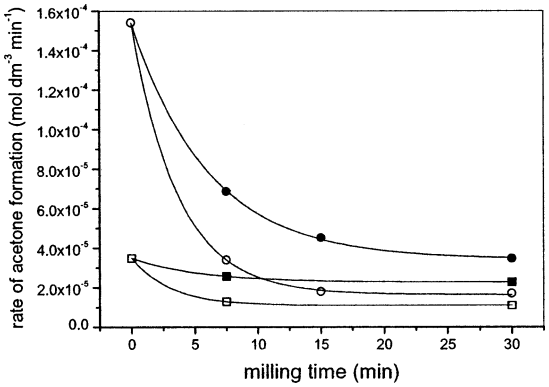

Figure 11. Comparison of experimental and calculated rates of 2-propanol oxidation versus milling time for sample A and sample B. ● Measured rate for sample A, ○ calculated rate for sample A. ■ Measured rate for sample B, □ calculated rate for sample B.

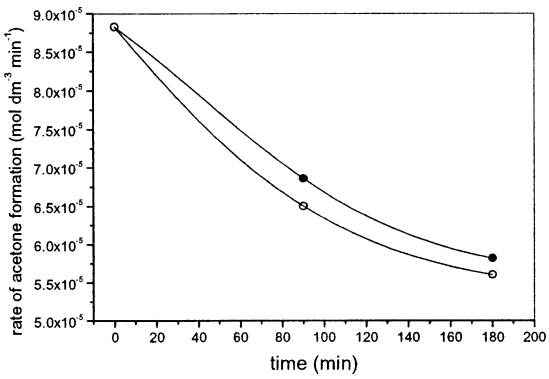

Figure 12. Comparison of experimental and calculated rates of 2-propanol oxidation versus milling time for sample C. ● Measured rate for sample C, ○ calculated rate for sample C.

oxidation rate are due only to changes in the UV penetration, i.e., that the rate of generation of charge carriers is equally efficient for all wavelengths. While this assumption is probably valid for the rutile samples,[4] it may be expected that for the mainly anatase, sample C, the longer wavelength would be less effective.

The comparative effect of milling on the three different TiO_2 samples was then compared. Since the results of the calculations, Table 4, are relatively insensitive to wavelength and since the maximum output of our lamp was at ~350 nm, this comparison has been made on the basis of the measured UV transmission at 350 nm. The results are shown in Figure 11, for sample A and B, and Figure 12 for sample C. In each case, the measured oxidation activity of milled suspensions (the solid points) is compared with the value calculated on the basis of applying the procedure outlined above to the result for the unmilled suspension.

The plots of Figures 11 and 12 show that, for all three types of TiO_2, even the simple model described above predicts changes in measured photoactivity that are comparable with, though larger than, the measured changes. The quantitative fit is best for sample C, for which the calculated decrease of 36% compares with a measured decrease of 33%. This is remarkable agreement since the calculation is simply based on the wavelength of maximum output of the UV lamp and does not take into account the spectral distribution. For sample A, the calculated decrease of 88% compares with a measured decrease of 78%, but for sample B, the calculated decrease of 69% is significantly greater than the measured value of 35%. The poor quantitative correspondence between calculated and measured values for milled suspensions of B probably occurs because the relative errors in our estimates of UV penetration depth from transmission measurements are of greatest relative importance when the overall changes in penetration depth are small.

As referred to above, Heller and co-workers[15] measured a reduction of photoactivity of 0.2 μm TiO_2 particles heavily ball-milled by alumina grinding materials for many days. The particles were of pigmentary origin and contained aluminum oxide in their surface which had been treated with triethanolamine. Milling for 3 days led to a 45% drop in photoactivity, and milling for 21 days led to a 90% drop in photoactivity and was associated with a reduction of BET derived particle size from 0.2 to 0.1 μm. The reduction in photoactivity was attributed to the introduction of bulk defects associated with the milling/grinding. Although we do not consider that Heller's explanation is relevant to our results, it is appropriate to list the reasons for our conclusion. First, the milling in Heller's experiments was much more severe than in the present studies. While large grinding media and consequent mechanic stress might well induce bulk defects at which electrons and holes can recombine, the much milder conditions (200 μm ballotini cf. 6 mm alumina cylinders) used in our experiments were specifically chosen so as not to induce crystal fracture of the type caused by Heller. This difference is also demonstrated in the dependence of measured photoactivity on milling time. In our experiments, the effect of milling had reached a limiting value after 30 min, in Heller's, photoactivity continued to fall as the milling time was increased from 14 to 21 days. Second, in the nanoparticles used by us, the relative importance of surface recombination relative to bulk recombination would be much greater than for the pigmentary samples used by Heller. Therefore, any effects of mechanical stress would be proportionately less. Third, the semiquantitative agreement between our experimental measurements and the calculations based on our rather simple model strengthen our confidence in the essential correctness of our interpretation for our nano-particulate suspensions.

Conclusion

The conclusion of this study is that the results of photo-oxidation measurements made on a simple organic molecule by slurries of particulate titanium dioxide under fixed experimental conditions (catalyst concentration, UV source, cell optics, etc.) are sensitive to the state of dispersion of the TiO_2. This

sensitivity arises because changes in the optics induce a different distribution of absorbed photons between the many particles which constitute the total reaction system. Because of the $I^{0.5}$ dependence of reaction rate on light intensity, the absorption of photons by fewer particles is not fully compensated by the increased oxidation rate at the surface of those particles. Further, the result has been confirmed by measurements (to be reported elsewhere) of oxidation of nitrophenol confirming that the conclusion is not a trivial consequence of some detail of the 2-propanol oxidation mechanism.

The conclusion is important because it affects any comparison of photoactivity of different TiO_2 samples when measured in a fixed reaction. Since the catalyst dispersion depends on the medium in which it is suspended, the results are also highly relevant to comparisons of the activity of a catalyst slurry in two different reactions or of the relative activities of catalysts for two or more photoreactions.

Acknowledgment. The authors thank the Solaveil Business of ICI Uniqema and the EPSRC for the provision of a CASE award under which this work was carried out. They are grateful to Dr. G. P. Dransfield, Dr. L Kessell, Mrs. S. Cutter, and all of Solaveil for the provision of samples and continued helpful discussions. It is a pleasure to thank Mr. D. F. Tunstall for advice on the optics of particulate dispersions and Dr. R. Buscall (ICI) for pointing out an error in their original analysis of the results.

References and Notes

(1) Mills, A.; Le Hunte, S. *J. Photochem. Photobiol., A* **1997**, *1*, 108.
(2) Ollis, D.; El-Akabi, H. *Photocatalytic Purification and Treatment of Water and Air*; Elsevier: New York, 1993.
(3) Tryk, A. D.; Fujishima, A.; Honda, K. *Electrochim. Acta* **2000**, *45*, 2363.
(4) King, C. J.; Egerton, T. A. *J. Oil Col. Chem. Assoc.* **1979**, *62*, 386.
(5) Egerton, T. A. *Kirk Othmer Encyclopedia of Chemical Technology*, 4th ed.; John Wiley & Sons: New York, 1997; Vol. 24, p 225.
(6) Gratzel, M.; O'Regan, B. *Nature (London)* **1991**, *353*, 737.
(7) Crittenden, J. C.; Zhang, Y.; Hand, D. W. *Water Environ. Res.* **1996**, *68*, 270.
(8) Christensen, P. A.; Walker, G. M. *Opportunities for the UK in Solar Detoxification, ETSU s/P4/00249/REP*; H. M. S. O.: London 1996.
(9) Matsunaga, T.; Tomoda, R.; Nakajima, T.; Wake, H. *Microbiology. Lett*. **1985**, *29*, 211.
(10) Matsunaga, T.; Nakajima, T.; Tomada, R.; Wake, H. *FEMS Microbiol. Lett.* 211.10.
(11) Wei, C.; Lin, W. Y.; Zulkarnain, Z.; Williams, N. E.; Zhu, K.; Kruzic, A. P.; Smith, R. L.; Rajeshawar, K. *Environ. Sci. Technol.* **1994**, *28*, 934.
(12) Bolton, J. R.; Sun, L. Z. *J. Phys. Chem.* **1996**, *100*, 4127.
(13) Cundall, R. B.; Rudham, R.; Salim, M. S. *J. Chem. Soc., Faraday Trans. 1* **1976**, *72*, 1642.
(14) Ramis, G.; Busca, G.; Lorenzeolli, V. *J. Chem. Soc., Faraday Trans. 1* **1987**, *83*, 1591.
(15) Heller, A.; Degani, Y.; Johnson D. W.; Gallagher, P. K. *J. Phys. Chem*. **1987**, *91*, 5987.
(16) Zhang, Z.; Wang, C.; Zakaria, R.; Ying, J. *J. Phys. Chem. B* **1998**, *102*, 10871.
(17) Torimoto, T.; Nakamura, N.; Ikeda, S.; Ohtani, B. *Phys. Chem. Chem. Phys*. In press.
(18) Boonstra, A. H.; Mutsaers, C. A. H. A. *J. Phys. Chem*. **1975**, *79*, 1694.
(19) Yu, J. G.; Zhao, X. J.; Zhao, Q. N. *Thin Solid Films* **2000**, *7*, 379.
(20) Stark, W. J.; Pratsinis, S. E.; Baiker, A. *Chimia* **2002**, *56*, 485.
(21) Karvinen, S. M. *Ind. Eng. Chem. Res*. **2003**, *42*, 1035.
(22) Egerton, T. A.; Tooley, I. R. *J. Mater. Chem*. **2002**, *12*, 1111.
(23) Emeline, A.; Salinaro, A.; Serpone, N. J. *Phys. Chem*. **2000**, *104*, 11202.
(24) Rudham, R.; Ward, S. J. *J. Chem. Soc., Faraday Trans. 1* **1983**, *79*, 1381.
(25) Parfitt, G. D. *Dispersion of Powders in Liquids*, 2nd ed.; Applied Science Publishers: Barking, U.K., 1973.
(26) Bickley, R. I.; Stone, F. S. *J. Catal*. **1973**, *31*, 389.
(27) Fraser, I. M.; MacCallum, J. R. *J. Chem. Soc., Faraday Trans. 1* **1986**, *82*, 607.
(28) Wamer, W. G.; Yin, J. J.; Wie, R. R. *Free Radical Biol. Med*. **1997**, *23*, 851.
(29) Hirakawa, T.; Kominami, H.; Ohtani, B.; Nosaka, Y. *J. Phys. Chem.* **2001**, *105*, 6993.
(30) Blount, M. C.; Buchholz, J. A.; Falconer, J. L. *J. Catal*. **2001**, *197*, 303.
(31) Fraser, I. M.; MacCallum, J. R. *J. Chem. Soc., Faraday Trans. 1* **1986**, *82*, 2747.
(32) Tunstall, D. F. U.K. Patent 2,046,898.
(33) Egerton, T. A.; Tetlow, A. In *Titanium Dioxide Products in Industrial Inorganic Chemicals Production and Uses*; Thompson, R., Ed.; Royal Society of Chemistry: Cambridge, U.K., 1995.
(34) Bohren, C. F.; Huffman, D. R. *Absorption and Scattering by Small Particles*; Wiley-Interscience: New York, 1998.
(35) Tunstall, D. F. *J. Cosmet. Sci*. **2000**, *51*, 303.
(36) Tunstall, D. F. Personal communication.